

MESCon 2014 [4th -5<sup>th</sup> September 2014]  
National Conference on Material for Energy Storage and Conversion- 2014

## Synthesis of titanium dioxide nanostructures and their effects on current-voltage (I-V) performance in dye sensitized solar cells

R. Govindaraj<sup>1</sup>, M. Senthil Pandian<sup>1</sup>, P. Ramasamy<sup>1\*</sup>,  
Sumita Mukhopadhyay<sup>2</sup>

<sup>1</sup>SSN Research Centre, SSN College of Engineering, Chennai-603 110,  
Tamilnadu, India

<sup>2</sup>Centre for Excellence for Green Energy and Sensor System, Indian Institute of  
Engineering Science and Technology, Howrah, West Bengal-711 103, India

\*Corres.author: ramasamp@ssn.edu.in

**Abstract :** Anatase phase TiO<sub>2</sub> nanostructures (Nanoparticles and nanorods) were prepared by two different methods. The prepared samples were characterized with Powder X-ray diffraction (PXRD), Field emission scanning electron microscopy (FESEM), High resolution transmission electron microscopy (HRTEM), Brunauer-Emmett-Teller (BET) method and Barrett-Joyner-Halenda (BJH) analysis. The PXRD pattern shows that both the nanostructures are anatase phase with good crystalline nature. The morphological results show that the TiO<sub>2</sub> nanorods have diameter of about ~ 25 nm and the length of ~ 100 nm. The TiO<sub>2</sub> nanoparticles are spherical in shape with mesoporous property. The solar energy conversion efficiency ( $\eta$ ) of the cell using nanoparticles with mesoporous structure was about 3.415 % with Jsc of 13.206 mA/cm<sup>2</sup>, Voc of 0.607 V and FF of 43 % ; while efficiency of the cell using nanorods reached 1.21 % with Jsc of 4.35 mA/cm<sup>2</sup>, Voc of 0.661V and FF of 42%.

**Keywords:** Semiconductors, X-ray diffraction; Dye sensitized solar cells; mesoporous

### Introduction

Among the development of photovoltaic devices, dye-sensitized solar cells (DSSCs) have been recognized as the most important and promising candidate for low-cost and high energy conversion. In typical DSSCs, mesoporous TiO<sub>2</sub> nanoparticles were widely used as photoanodes to provide large internal surface area for anchoring enough dye loading. Nevertheless, further improvement in DSSC's performance has been limited by the random electrons pathway and short electron diffusion length (10–35  $\mu$ m) induced by excessive trapping and detrapping events occurring within large defects, surface states and grain boundaries of nanoparticles. The one-dimensional (1D) TiO<sub>2</sub> nanostructures such as nanorods, nanowires or nanotubes have been estimated to significantly increase the electron diffusion length up to 100  $\mu$ m for DSSC since they confer the advantages of providing direct electron transfer pathways and effectively inhibiting photo-generated charge recombination[1-7]. However, it has limited porous property of the photoanode, which cause to inefficient dye loading during the sensitization.

In this study, anatase phase TiO<sub>2</sub> nanorods and nanoparticles has been synthesized by hydrothermal and sol-gel method respectively. The synthesized materials were subjected to Powder X-ray Diffraction (PXR), Field Emission Scanning Electron Microscopy (FESEM), High Resolution Transmission Electron Microscopy (HRTEM), Selected Area Diffraction (SAED) Pattern, Brunauer-Emmett-Teller (BET) method and Barrett-Joyner-Halenda (BJH) method. In order to confirm the photovoltaic performance of the TiO<sub>2</sub> nanostructures in DSSC, the photocurrent-voltage (I-V) measurement were carried out with simulated solar light (Newport - Oriel instruments-100 mW/cm<sup>2</sup>).

## Experimental Procedure

### 1. Preparation of TiO<sub>2</sub> Nanoparticles (Sol-gel Method)

All the chemical reagents were used for synthesis of TiO<sub>2</sub> nanoparticles without further purification. The synthesized product was obtained from titanium (IV) isopropoxide (TTIP) dissolved in ethanol and certain amount of deionized water was added to the solution in molar ratio of Ti: H<sub>2</sub>O=1:4. The mixed solution was vigorously stirred for 1 hr in order to form sols. After aging for a day, the sols were transformed into gel form. The obtained gels were dried at 120 °C for 24 hr to remove the water and organic materials. After that, the dried gel was sintered at 450 °C for 2 hr in home-made high temperature programmable furnace. Finally the pure TiO<sub>2</sub> nanoparticles were obtained.

### 2. Preparation of TiO<sub>2</sub> Nanorods (Hydrothermal method)

Titanium (IV) butoxide (Aldrich) was mixed with the same amount of acetylacetone (ACA) to slowdown the hydrolysis and the condensation reactions. Subsequently 40 mL of Millipore water was slowly added into the solution, and stirred well for 5 min at room temperature. After kept stirring, aqueous ammonia solution (25-30%) 30 mL was slowly added drop by drop into the above solution, then the solution was transferred into a 250 mL Teflon-lined stainless steel autoclave vessel and placed in a silicone oil containing bath. Then the precursors containing solution is heated at 170 °C and kept for 3 days with stirring condition in the same temperature without any temperature fluctuation. After that, the autoclave was naturally cooled to room temperature. The obtained product was thoroughly washed with aqueous HCl solution, 2-Propanal and Millipore water for several times, followed by drying at 120 °C for 12 hr. Finally, the obtained samples were collected and calcined at 450 °C for 1 hr in homemade programmable high temperature furnace.

### 3. Fabrication Procedure for Dye Sensitized Solar Cells

The electrodes were prepared as follows: 1 g of TiO<sub>2</sub> powder was mixed with 0.1 mL of acetylacetone and ground mechanically. During vigorous stirring, 5 mL of mixture of water and ethanol (1:1 vol %) was added and 0.4 mL of polyoxethylene (10) octylphenyl ether (Triton x-100) was added with the above solution to form a paste. the obtained colloidal paste was coated on the FTO (Sheet resistanc,8 Ω□) substrate by doctor blade technique. After coating, the resulting film was sintered at 500 °C for 1 hr. The same procedure was followed for nanorods based photoanode. The sintered electrodes were soaked in 0.3 mM of cis-Bis(isothiocyanato) bis(2,2'-bipyridyl-4,4'-dicarboxylato ruthenium(II) (known as N3) dye in an ethanol solution. The counter electrode was prepared by doctor blade technique using Platisol T/SP (Solaronix SA) precursor and thermally decomposed at 400 °C for 30 min. Finally both electrodes are sandwiched together to form a cell. The small amount of electrolyte (Iodolyte AN-50) was injected into cell.

## Characterization

### Powder X-ray Diffraction Analysis

The formation of anatase phase and average crystallite size of TiO<sub>2</sub> nanostructures were evaluated by powder X-ray diffraction analysis. Figure. 1. shows the PXR pattern of TiO<sub>2</sub> nanostructures. The preferred orientation corresponding to the plane (101) is observed in the samples. All the diffraction peaks in the diffraction patterns can be indexed as anatase phase of TiO<sub>2</sub> nanoparticles and the diffraction pattern was in good agreement with JCPDS files # 21-1272 [8].

The dominant (101) peak shows that the anatase phase was formed in the synthesized materials. In order to quantify the particle size effects, we can estimate the mean crystallite size (D) of these samples by applying the Scherrer equation to the strongest (101) plane diffraction peak ( $2\theta=25^\circ$ )

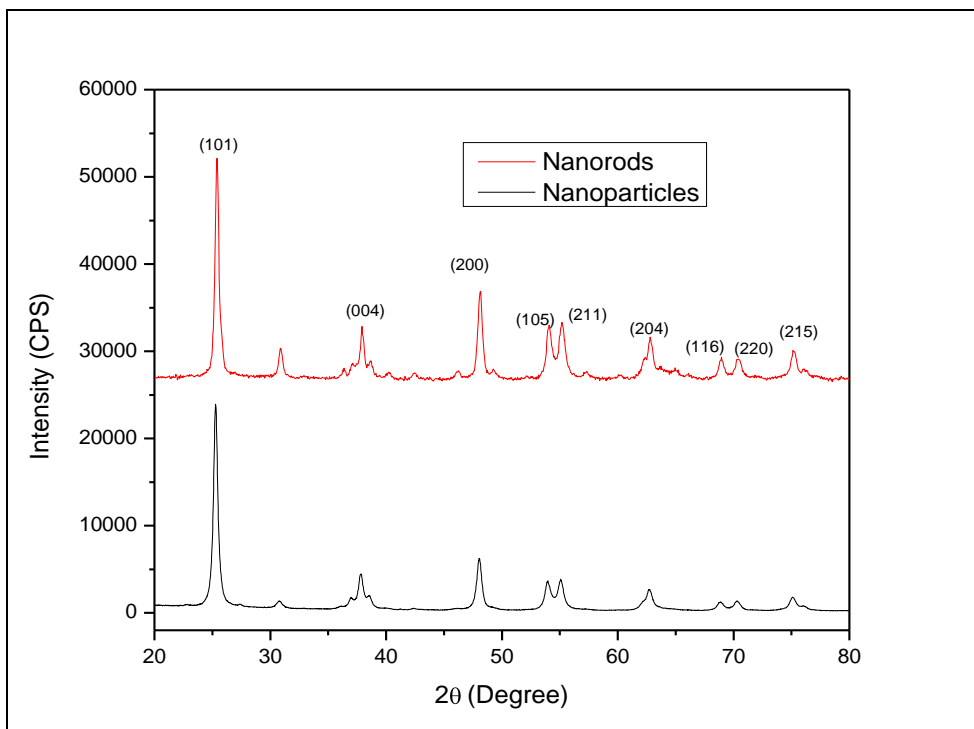


**Figure 1. Powder XRD pattern of TiO<sub>2</sub> nanostructures after calcined at 450 °C.**

$$D = 0.9 / (\beta \cos \theta)$$

where  $\lambda$  is the X-ray wavelength,  $\beta$  is the full width at maximum of the diffraction intensity and  $\theta$  is the Bragg angle. The mean crystallite size of the TiO<sub>2</sub> nanoparticles and nanorods are 20 nm and 17 nm respectively.

### **Nitrogen Adsorption and Desorption Isotherm of TiO<sub>2</sub> nanostructures and Nanorods**

The specific surface area and porosity of the mesoporous anatase TiO<sub>2</sub> nanoparticles were evaluated by using the nitrogen adsorption and desorption isotherms after sintering as shown in Figure 2a and Figure 2b. The isotherm of sample reveals the stepwise adsorption and desorption branch of type IV pattern, indicating the presence of mesoporous material having a three dimensional (3D) intersection according to the IUPAC classification. A hysteresis loop with a stepwise adsorption and desorption branch is observed at wide range of pressure (P/P<sub>0</sub>). The surface area of TiO<sub>2</sub> nanoparticles is 31.76 m<sup>2</sup>g<sup>-1</sup> as shown in Figure 2a. This result indicates that the synthesized material has wider mesoporous structure. To analyse pore size, the plots of the pore size distribution are investigated by desorption branch of the BJH method as shown in Figure 2b. The average pore diameters of mesoporous TiO<sub>2</sub> nanostructures are 7.1 nm and 9.3 nm. This kind of porous structure can be useful for efficient electrolyte diffusion into the photoanode in DSSC.

Figure 2c. shows the nitrogen adsorption and desorption isotherm and pore size distribution of the TiO<sub>2</sub> nanorods. The specific surface area and average pore width of the TiO<sub>2</sub> nanorods are 84.83 m<sup>2</sup>/g and 5.7 nm respectively. The isotherm exhibits type IV pattern with hysteresis loop, characteristic of mesoporous material according to the classification of IUPAC. A sharp increase in adsorption volume of N<sub>2</sub> was observed and located in the P/P<sub>0</sub> range of 0.67-0.99. The pore size distribution obtained by BJH approach (Figure 2d.) is noticeably narrow (5.7 nm), confirming good quality of the sample.

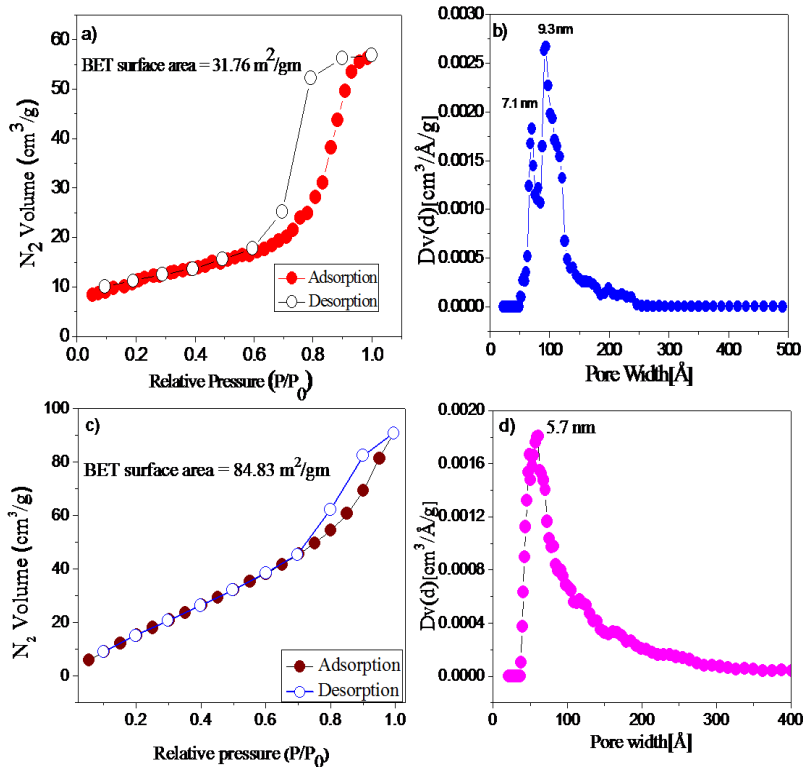


**Figure 2. Nitrogen Adsorption-Desorption isotherm of TiO<sub>2</sub> nanostructures . (a-b) BET surface area and pore size distribution of TiO<sub>2</sub> nanoparticles (c-d) BET surface area and pore size distribution of nanorods.**

### Morphology

Figure 3 (a-b). shows the FESEM and SAED pattern image of mesoporous TiO<sub>2</sub> nanoparticles calcined at 450 °C. The morphology of synthesized material is spherical in shape. Discernable pores are present at the surface of mesoporous TiO<sub>2</sub>. The pore structure is observed at the space between TiO<sub>2</sub> nanoparticles, indicating that the interparticle porosity is due to the mesoporosity. From the FESEM analyses, the mechanism for the formation of mesoporous TiO<sub>2</sub> can be analyzed. As can be seen from the FESEM images, the mesoporous TiO<sub>2</sub> probably arises from the aggregation of nanocrystalline TiO<sub>2</sub> particles.

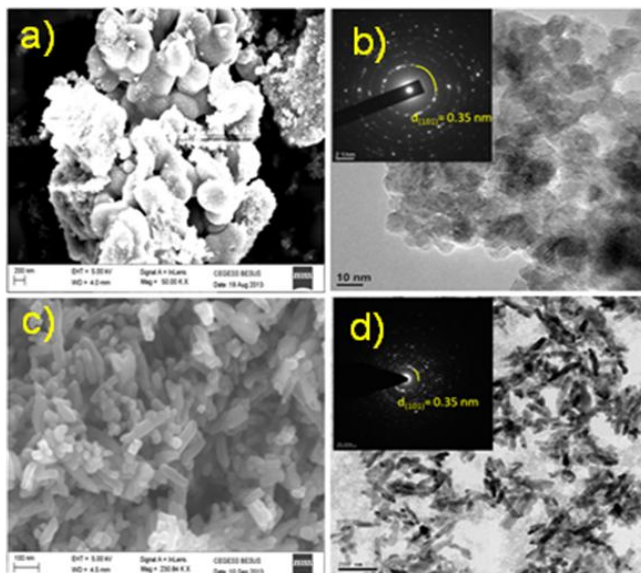


**Figure 3. Morphological images of TiO<sub>2</sub> nanostructures: (a-b) FESEM image and SAED pattern of TiO<sub>2</sub> nanoparticles. (c-d) FESEM image and SAED pattern of TiO<sub>2</sub> nanorods.**

When the titanium precursor was dissolved in ethanol, TiO<sub>2</sub> nanoparticles can be formed via hydrolysis and condensation process. Further hydrolysis and condensation of titanium precursors lead to the growth of larger TiO<sub>2</sub> nanoparticles, which are slowly aggregated to one another. As TiO<sub>2</sub> nanoparticles are further aggregated, the TiO<sub>2</sub> particles become microscopic particles, and finally form microspheres as shown in Figure 3a. Selected area diffraction is shown in Figure 3b, which clearly indicates that the TiO<sub>2</sub> nanoparticles are highly crystalline in nature with anatase phase ( $d=0.35$  nm).

Figure 3c. shows the FESEM images of synthesized nanorods, indicating the nanorods-like morphology composed of different size rods. The rods structure had approximately 25 nm diameters and 100 nm length. SAED pattern (Figure 3d.) confirms the anatase phase ( $d_{(101)}=0.35$  nm) with PXRD.

### I-V Characteristics

The photocurrent–voltage curve (I–V) measurements were performed with an AM 1.5G solar simulator (Newport–Oriol). Xenon arc lamp served as the light source, whose incident light intensity was calibrated with a NREL-calibrated Si solar cell equipped with an optical filter to approximate AM 1.5G one sun light intensity (100 mW/cm<sup>2</sup>) before each measurement.

**Table:1 Photovoltaic properties of DSSC**

Cell	Jsc (mA/cm <sup>2</sup> )	Voc (V)	Fill Factor (%)	Efficiency (η %)
Nanoparticles	13.206	0.607	43	3.415
Nanorods	4.35	0.661	42	1.21

Figure 4. shows the I-V characteristics of the solar cells. The Sol-gel synthesized TiO<sub>2</sub> nanoparticles exhibit better conversion efficiency than hydrothermal nanorods. The improvement of efficiency in sol-gel based TiO<sub>2</sub> nanoparticles could be due to the more porous nature of the particles. As per BET analysis, the surface area of the TiO<sub>2</sub> nanoparticles is 31.76 m<sup>2</sup>/g, which is significantly lower than nanorods (83.84 m<sup>2</sup>/g). However, the pore width of the nanoparticles is relatively larger than nanorods (nanoparticles-9.1 nm and nanorods-5.3 nm). So, this can help for better electrolyte diffusion to regenerate the dye molecules.

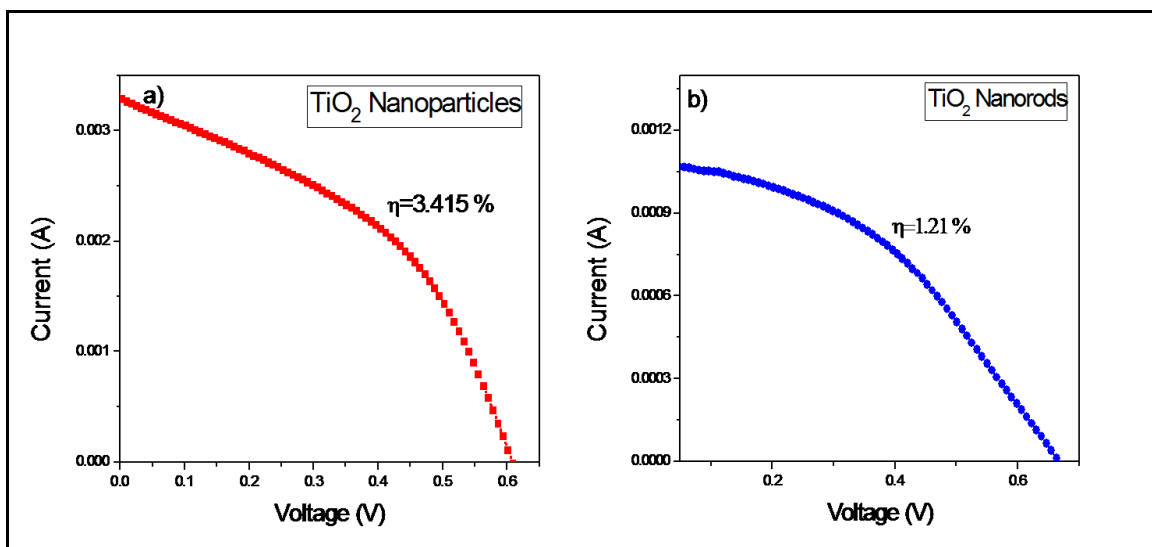


**Figure 4. I-V performance of the nanostructures: a. TiO<sub>2</sub> nanoparticles and b. TiO<sub>2</sub> nanorods.**

### Conclusion

The mesoporous TiO<sub>2</sub> nanoparticles and nanorods were successfully synthesized with Sol-gel and hydrothermal method respectively. The obtained nanostructures have anatase phase, which is confirmed with powder XRD and it also shows good crystalline behavior of the samples. The morphological properties were identified with FESEM analysis. The surface area and pore size distribution of the nanostructures were analyzed

with BET and BJH method. The photovoltaic performances of the TiO<sub>2</sub> nanostructures were carried out. The photoconversion efficiency of the TiO<sub>2</sub> nanoparticles is 3.415 %, while the efficiency of the nanorods is 1.21 %. The performance of the TiO<sub>2</sub> nanoparticles is reasonably better than nanorods. This could be due to the large pore size in the nanoparticles in the photoanode.

### Acknowledgments

The authors would like to express gratitude to Prof. A. K. Barua, IEST, Howrah, West Bengal for all the encouragement. The authors thank National Centre for Nanosciences and Nanotechnology, Medras University, Chennai for microscopy studies.

### References

1. Liao. J. Y, Lei B. X, Kuang. D. B, and Su. C. Y, Tri-functional hierarchical TiO<sub>2</sub> spheres consisting of anatase nanorods and nanoparticles for high efficiency dye-sensitized solar cells, *Energy Environ.Sci.*, 2011, 4, 4079-4085.
2. Wu. W. Q, Liao. J. Y, Chen. H. Y, Yu. X. Y, Su. C. Y and Kuang. D. B, Dye-sensitized solar cells based on a double layered TiO<sub>2</sub> photoanode consisting of hierarchical nanowire arrays and nanoparticles with greatly improved photovoltaic performance, *J. Mater. Chem.*, 2012, 22, 18057-18062.
3. Fisher. A. C, Peter. L. M, Ponomarev. E. A, Walker. A. B and Wijayantha. K. G. U, Intensity Dependence of the Back Reaction and Transport of Electrons in Dye-Sensitized Nanocrystalline TiO<sub>2</sub> Solar Cells, *J. Phys. Chem. B*, 2000,104, 949-958.
4. Du. J, Qi. J, Wang. D, and Tang. Z, Facile synthesis of Au@TiO<sub>2</sub> core-shell hollow spheres for dye-sensitized solar cells with remarkably improved efficiency *Energy Environ. Sci.*, 2012,5, 6914-6918.
5. Li. Y, Wang. H, Feng. Q. Y, Zhou. G, and Wang. Z. S, Gold nanoparticles inlaid TiO<sub>2</sub> photoanodes: a superior candidate for high-efficiency dye-sensitized solar cells, *Energy Environ. Sci.*, 2013, 6, 2156-2165.
6. Jennings. J. R, Ghicov. A, Peter. L. M, Schmuki. P, Walker. A. B, Dye-Sensitized Solar Cells Based on Oriented TiO<sub>2</sub> Nanotube Arrays: Transport, Trapping, and Transfer of Electrons *J. Am. Chem. Soc.*, 2008, 130, 13364-13372.
7. Zhang. D. R, Cha. H.G, and Kang. Y. S, Hydrothermal synthesis of anatase TiO<sub>2</sub> nanorods with high crystallinity using ammonia solution as a solvent, *J Nanosci Nanotechnol.* 2011, 11, 6007-6012.
8. Xu. J, Li. L, Yan. Y, Wang. H, Wang. X, Fu. X, and Li. G, Synthesis and photoluminescence of well-dispersible anatase TiO<sub>2</sub> nanoparticles, *J. Colloid and interface Science* 2008, 318, 29-34.

\*\*\*\*\*